

An Efficient Global Optimization Algorithm with Adaptive Estimates of the Local Lipschitz Constants

Danny D'Agostino 

the date of receipt and acceptance should be inserted later

Abstract In this work, we present a new deterministic partition-based Global Optimization (GO) algorithm that uses estimates of the local Lipschitz constants associated with different sub-regions of the domain of the objective function. The estimates of the local Lipschitz constants associated with each partition are the result of adaptively balancing the global and local information obtained so far from the algorithm, given in terms of absolute slopes. We motivate a coupling strategy with local optimization algorithms to accelerate the convergence speed of the proposed approach. In the end, we compare our approach HALO (Hybrid Adaptive Lipschitzian Optimization) with respect to popular GO algorithms using hundreds of test functions. From the numerical results, the performance of HALO is very promising and can extend our arsenal of efficient procedures for attacking challenging real-world GO problems. The Python code of HALO is publicly available on GitHub.¹

Keywords Global Optimization · Lipschitz Optimization · Black-box Optimization

1 Introduction

In this work, we consider the following optimization problem

$$\begin{aligned} \min_{\mathbf{x}} f(\mathbf{x}) \\ \text{subject to: } \mathbf{x} \in \mathcal{D} \end{aligned} \tag{1}$$

where $f : \mathbb{R}^N \rightarrow \mathbb{R}$, $\mathbf{x} \in \mathbb{R}^N$ and \mathcal{D} is the feasible region of \mathbb{R}^N , defined by box constraints $\mathcal{D} = \{\mathbf{x} \in \mathbb{R}^N : \mathbf{l} \leq \mathbf{x} \leq \mathbf{u}\}$. The N -dimensional vectors \mathbf{l} and \mathbf{u} represent the lower and upper bound on the decision variable \mathbf{x} .

Global Optimization (GO) is the field of Operations Research where methodologies and algorithms are developed to find the global optimal solution of Problem 1. The

National University of Singapore
Department of Industrial Systems Engineering and Management
Singapore
E-mail: dannydag@nus.edu.sg

¹ <https://github.com/dannyzx/HALO>

importance to obtain the best overall solution for a specific problem is so fundamental and crucial that spans any field of science.

For this reason, years of intense academic research have been dedicated to GO and many approaches have been proposed. Stochastic and Evolutionary algorithms as the Controlled Random Search [1], Genetic Algorithm [2], Simulated Annealing [3], Particle Swarm Optimization [4] and Covariance Matrix Adaptation Evolutionary Strategy [5] are known to have been effective in many real-world applications.

A different class of GO algorithms is the ones that construct a response surface of the objective function through statistical models such as Gaussian Processes [6, 7] or Radial Basis Functions [8, 9]. These methodologies, in the case the objective function f is very expensive to evaluate, demonstrated to provide a good reduction in objective function value in a very limited number of function evaluations.

Another class of GO algorithms is Lipschitz Optimization which is extensively studied and developed in the last decades [10][11][12] [13] [14].

In Lipschitz Optimization, we assume that the objective function f to be *Lipschitz continuous* on the feasible domain \mathcal{D} which means that a constant value in $0 < L < \infty$ exists such that

$$|f(\mathbf{x}) - f(\bar{\mathbf{x}})| \leq L\|\mathbf{x} - \bar{\mathbf{x}}\| \quad \forall \mathbf{x}, \bar{\mathbf{x}} \in \mathcal{D} \quad (2)$$

where L is the global Lipschitz constant of the function f and $\|\cdot\|$ is the Euclidean norm (different norms can also be used as analyzed in [15]). The requirement for f to be Lipschitz-continuous is not particularly restrictive, indeed this class of functions is very general because a continuously differentiable function defined into a convex and compact set is always Lipschitz continuous [14]. In this case the Lipschitz constant L is given by the maximum norm of the gradient $L = \max_{\mathbf{x} \in \mathcal{D}} \|\nabla f(\mathbf{x})\|$. The Lipschitz continuity of the objective function f is an important assumption because if we know the Lipschitz constant L we can compute valid lower bounds of f across its domain \mathcal{D} . In fact, knowing the function value at the point $f(\bar{\mathbf{x}})$, then we can compute the lower-bound for any $\mathbf{x} \in \mathcal{D}$ such that the following equation is valid

$$f(\bar{\mathbf{x}}) - L\|\mathbf{x} - \bar{\mathbf{x}}\| \leq f(\mathbf{x}) \quad (3)$$

and such information can be exploited from an algorithmic point of view to design efficient numerical procedures to seek the global optimum solution of Problem 1.

2 Related Work

During the years, researchers developed Lipschitz Optimization methods as in [16, 17] that given the value of the Lipschitz constant L , can produce valid lower bounds of the objective function f and driving the numerical procedure towards the global minimizers.

The difficulty is when the value L of the Lipschitz constant is not available in advance such as in the majority of real-world applications. To effectively overcome this issue, an estimation of it is usually carried out given the information acquired by the optimization procedure during its iterations as in [12].

A popular method that cleverly avoids any estimation of the Lipschitz constant L is the DIRECT (DIviding RECTangles) algorithm [18], a partition-based derivative-free for GO problems. The remarkable feature of the DIRECT algorithm, is in the concept of the *potentially optimal rectangles*, where any value of the global Lipschitz constant L with $L \in (0, \infty)$ is implicitly assumed when selecting the partitions to

explore. The other algorithmic interesting features of DIRECT are the simplicity of its partition scheme, the so-called everywhere dense property that ensures convergence at the global optimal solution as the algorithm iterates indefinitely, and the lack of important hyperparameters to set; in fact, DIRECT has only one hyperparameter and demonstrated to be quite robust respect to that in practice [18]. For those reasons, it inspired many other algorithms of that kind based on the idea of potentially optimal partitions [19, 20, 21, 22, 23, 24, 25, 26].

Other efficient and interesting algorithms in the class of Lipschitz Optimization, put efforts into the estimation of the local Lipschitz constant L_i for each sub-region \mathcal{D}_i of the domain \mathcal{D} . The algorithm presented in [27] is proposed for the optimization of univariate functions and for multivariate functions is used a dimensionality reduction method through Peano curves [28, 29]. In [30] the estimation of the local Lipschitz constants is used inside an efficient diagonal partition-based algorithm. In [31] the computation of the local Lipschitz constants is embedded in a scheme that reduces the initial multidimensional problem to a set of univariate subproblems connected recursively and also adaptively in [32]. In a similar concept, it has been proposed also in case the first derivative is available [33]. The performance of these approaches is highly sensitive to a reliability parameter that the user must fix before running the algorithm, as also highlighted in [30, 31, 34].

It is also applied with success, the hybridization of some of the approaches mentioned above with some local optimization methods. For example, the DIRECT algorithm has been hybridized with a globally convergent truncated Newton method in [35] and a coordinate descent in [36], showing enhanced performance as in [21].

3 Main Contribution

In this work, we provide an adaptive procedure to estimate the local Lipschitz constant associated with each partition \mathcal{D}_i . Our estimate is a result of a convex combination given by the absolute variation of the objective function around the partition \mathcal{D}_i and the current estimate of the global Lipschitz constant L . The coefficients in the convex combination, depending on the size of partition \mathcal{D}_i so that the estimates are adaptively and automatically computed and no hyperparameters must be defined apriori by the user. Based on the information of the local Lipschitz constants, we propose our criteria to select the most promising partitions, which completely set aside the concept of potentially optimal hyperrectangles of the DIRECT algorithm.

The asymptotic convergence of the algorithm to a global minimum is also established, ensuring that the so-called everywhere dense property. In HALO (Hybrid Adaptive Lipschitzian Optimization) we adopt the same partition strategy defined in the DIRECT algorithm and we will briefly highlight its features. Later, we introduce our adaptive estimation of the derivatives which is simply based on the application of the finite differences formulas with respect to the points sampled so far by the algorithm.

To accelerate the convergence speed of HALO towards stationary points, we show and motivate a simple coupling strategy with two different local optimization algorithms [37, 38].

In the end, we compare the performance of HALO with respect to popular GO algorithms as DIRECT [18], CMA-ES [5] and the hybridization of DIRECT namely DIRMIN [36]. We carried out a large numerical campaign to evaluate the algorithms using popular test functions as collected in [39] and two different test functions generators

specifically for GO problems presented in [40, 41], so that we considered more than one thousand test functions.

The numerical results show that HALO is very competitive and can extend our arsenal of efficient procedures for attacking challenging real-world GO problems.

4 HALO: Hybrid Adaptive Lipschitzian Optimization

Before diving into the details of HALO, could be necessary to describe its main steps from a macroscopic point of view and by introducing some notations.

The algorithm defined in 1 is composed by 3 parts: a main program, a selection and a partitioning step. The main program takes as input termination criteria, for now,

Algorithm 1: General Partition Algorithm for GO

```

1 function Main(MaxIter,  $\mathcal{D}$ )
2   for  $k$  to MaxIter do
3      $\mathcal{I}_k^* \leftarrow \text{Selection}(\mathcal{I}_k)$ 
4     for  $i_k^*$  in  $\mathcal{I}_k^*$  do
5       for  $j$  to  $J$  do
6          $\mathbf{x}_{i_k^*}^j \leftarrow \mathbf{x}_{i_k^*}^j \in \mathcal{D}_{i_k^*}$ 
7          $f(\mathbf{x}_{i_k^*}^j) \leftarrow \text{Fun\_Eval}(\mathbf{x}_{i_k^*}^j)$ 
8        $\mathcal{I}_k \leftarrow \text{Partitioning}(\mathcal{D}_{i_k^*})$ 
9   return  $\mathcal{I}_k^*$ 
10 function Selection( $\mathcal{I}_k$ )
11    $\mathcal{I}_k^* \leftarrow \mathcal{I}_k \subseteq \mathcal{I}_k$ 
12   return  $\mathcal{I}_k^*$ 
13 function Partitioning( $\mathcal{D}_{i_k^*}$ )
14    $\mathcal{D}_{i_k^*} \leftarrow \bigcup_{j=1}^J \mathcal{D}_{i_k^*}^j$ 
15    $\mathcal{I}_k \leftarrow \mathcal{I}_k \cup \{|\mathcal{I}_k| + j\}_{j=1}^J$ 
16   return  $\mathcal{I}_k$ 

```

represented by the maximum number of iterations and the box domain \mathcal{D} . In the first loop in line 2 the algorithm starts. At line 3, we select the partitions through some criteria not yet specified but it should somehow push the algorithm in regions where f is more likely to have the global minimum. Choosing a partition (or more than one), means selecting a subset of indices \mathcal{I}_k^* from the set of indices \mathcal{I}_k which contains the index i_k associated to each partition \mathcal{D}_{i_k} at iteration k .

At lines 4 and 5 we have two for loops: the outer one with respect to every index i_k^* of each selected partition, while the inner loop is used to perform J function evaluations inside each of them. At line 8, once the inner loop has terminated, the set $\mathcal{D}_{i_k^*}$ is divided into J non-overlapping subsets (line 14), which means the following

$$\mathcal{D}_{i_k^*}^j \subset \mathcal{D}_{i_k^*} \quad j = 1, \dots, J \quad (4)$$

At line 15, the set of indices \mathcal{I}_k is updated and the process described so far is repeated until the stopping criteria are met.

4.1 Selection

In the previous section, we described a general partition scheme for GO. Now, we start to add more details to the algorithm. In the first paragraph, we introduce our approach to estimating the local Lipschitz constant associated with every partition. In the second paragraph, given the values of the local Lipschitz constants, we describe how the partition is selected.

4.1.1 Adaptive Estimation of the Local Lipschitz Constants

In Lipschitz optimization, in general, the strategy is to obtain the information about the Lipschitz constant L , to compute the lower bounds of the objective function f , and drive the algorithm in regions where those lower bounds are lower. The main concern about using the global Lipschitz constant estimates is that sometimes could be a poor indication of the behavior of the objective function in some particular region of the domain \mathcal{D} .

For example, if a function f is flat almost everywhere but there is a little region of \mathcal{D} where the behavior of f is highly chaotic (i.e. higher Lipschitz constant), then the resulting lower bounds computed around the region of the domain \mathcal{D} where f has a gentler behavior could result in a poor estimate of them. This is because the global Lipschitz constant represents only the overall maximum variation of the objective function f . Thus, the estimation of the local Lipschitz constant \tilde{L}_i associated with each partition \mathcal{D}_i would be significantly more informative than the global Lipschitz constant L .

Therefore, it is necessary to introduce a local source of information about the function f when estimating the lower bounds of the objective function. This local source of variation can be represented by the norm of the gradient at the centroid \mathbf{x}_i . But in our case we want to maintain the overall procedure derivative-free and indeed the exact form of the gradient is supposed to be unknown (as the objective function f). In this work, we are going to approximate the gradient around every centroid \mathbf{x}_i of each partition \mathcal{D}_i by only using the points sampled so far by the algorithm. Then, the accuracy in the computation of all the gradients depend directly on the size of each partition.

Is reasonable to think that as the size of a partition \mathcal{D}_i decrease also the uncertainty about the behavior of the objective function around \mathcal{D}_i decreases. Then makes sense to balance automatically the value of our estimate of the local Lipschitz constant \tilde{L}_i based on the size of its relative partition \mathcal{D}_i . More specifically we propose the following adaptive formula

Definition 4.1 Given \mathcal{D}_{i_k} a partition of the feasible space at iteration k and given

$$\alpha_{i_k} = \frac{\|\mathbf{u}_{i_k} - \mathbf{l}_{i_k}\|}{\sqrt{N}} \quad \alpha_{i_k} \in (0, 1), \quad \tilde{L}_k = \max_{i_k \in \mathcal{I}_k} \|\tilde{\nabla} f(\mathbf{x}_{i_k})\| \quad (5)$$

then the relative estimation of the local Lipschitz constant L_{i_k} is given by

$$\tilde{L}_{i_k} = \alpha_{i_k} \tilde{L}_k + (1 - \alpha_{i_k}) \|\tilde{\nabla} f(\mathbf{x}_{i_k})\| \quad (6)$$

In Eq. 6, the term α_{i_k} is given by the ratio between the diagonal of the partition \mathcal{D}_{i_k} and the main diagonal of the feasible set \mathcal{D} that is \sqrt{N} , in case the domain

is normalized into a unit hypercube. As the diagonal of the partition \mathcal{D}_{i_k} namely $\|\mathbf{u}_{i_k} - \mathbf{l}_{i_k}\|$ decreases, then the local information in the neighbour of \mathcal{D}_{i_k} becomes more precise and the estimate of the local Lipschitz constant is mainly given by the norm of the approximation of the gradient at \mathbf{x}_{i_k} namely $\|\tilde{\nabla}f(\mathbf{x}_{i_k})\|$. Otherwise, if the diagonal of the partition \mathcal{D}_{i_k} is approximately equal to the maximum diagonal, then the local information could not be reliable and the estimate of the local Lipschitz constant, in this case, is mainly given by the estimate of the global Lipschitz constant \tilde{L}_k , that represents the maximum absolute variation obtained during the algorithm iterations.

In the following section, we define the criteria for selecting the partitions \mathcal{D}_{i_k} , given information collected in our estimates of local Lipschitz constants.

4.1.2 Selection Criteria

In the following definition, we show which partitions \mathcal{D}_{i_k} are selected in HALO

Definition 4.2 Given the estimation of the local Lipschitz constant \tilde{L}_{i_k} for every $i_k \in \mathcal{I}_k$ from Eq. 6, then the partition \mathcal{D}_{i_k} is selected if at least one of the following conditions is satisfied

Condition 1 if for $i_k \in \mathcal{I}_k$, then

$$f(\mathbf{x}_{i_k}) - \tilde{L}_{i_k} \|\mathbf{u}_{i_k} - \mathbf{l}_{i_k}\| \leq f(\mathbf{x}_{j_k}) - \tilde{L}_{j_k} \|\mathbf{u}_{j_k} - \mathbf{l}_{j_k}\| \quad \forall j \in \mathcal{I}_k \quad (7)$$

Condition 2 For $i_k \in \mathcal{I}_k$, then

$$f(\mathbf{x}_{i_k}) = f_{\min} \quad (8)$$

where $f_{\min} = \min_{j_k \in \mathcal{I}_k} f(\mathbf{x}_{j_k})$

Condition 3 if for $i_k \in \mathcal{I}_k^{\max}$ and

$$f(\mathbf{x}_{i_k}) - \tilde{L}_{i_k} \|\mathbf{u}_{i_k} - \mathbf{l}_{i_k}\| \leq f(\mathbf{x}_{j_k}) - \tilde{L}_{j_k} \|\mathbf{u}_{j_k} - \mathbf{l}_{j_k}\| \quad \forall j \in \mathcal{I}_k^{\max} \quad (9)$$

where $\mathcal{I}_k^{\max} = \{i_k \in \mathcal{I}_k : \|\mathbf{u}_{i_k} - \mathbf{l}_{i_k}\| = \max_{i_k \in \mathcal{I}_k} \|\mathbf{u}_{i_k} - \mathbf{l}_{i_k}\|\}$.

From Def. 4.2 a hyperrectangle is selected if satisfies at least one of three conditions.

With Condition 1, we select the hyperrectangle that obtains the lowest lower bound given the information collected in the local Lipschitz constant.

With Condition 2, we assure that the hyperrectangle with the lowest objective function value is also always selected. In this manner, in case HALO is used in high dimensional spaces with a very limited number of function evaluations allowed we can accommodate the user to find a decent local minimum. In general, we can expect that the information contained in the estimates of the local Lipschitz constant becomes more reliable as the partitions become smaller which is more challenging as the dimensionality N of the problem increases.

With Condition 3, among the hyperrectangles of maximum diagonal, we select the one that obtains the minimum lower bound. This choice has an important consequence from the algorithm convergence point of view as we will show in the next sections.

A graphical representation of our selection criteria can be found in Fig. 1. On the abscissa, we have the distance from the center to the vertices of each partition, and on the ordinate the relative function value. The slope of each line is given by the relative value of the estimated local Lipschitz constant \tilde{L}_{i_k} and highlighted in the color bar. A center \mathbf{x}_{i_k} of a partition associated with a high value of \tilde{L}_{i_k} is represented by a dot in a purplish color while a low value of \tilde{L}_{i_k} tends to be more yellowish. The selected

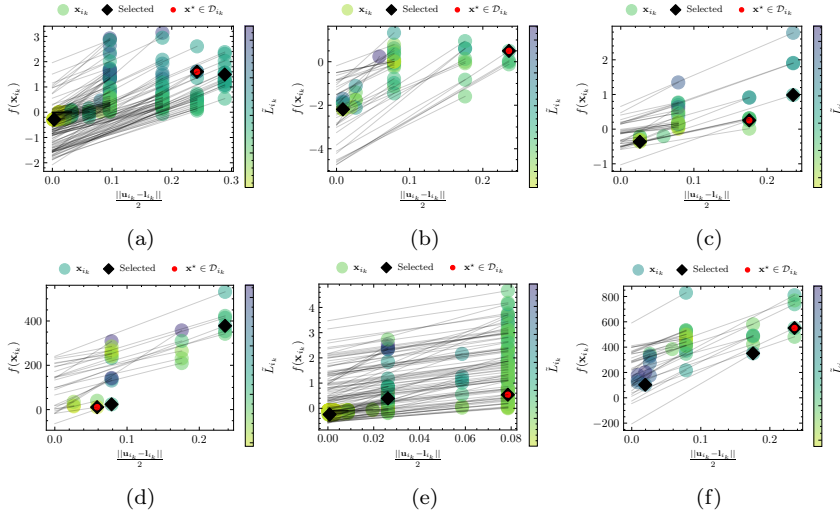


Fig. 1: Graphical representation of the selection criteria given in Def. 4.2.

partitions are marked with a black rhombus. The small red dot indicates in which partition the global minimum is located. It is possible to notice that HALO can take completely different trajectories from the DIRECT algorithm since all the potentially optimal hyperrectangles lie in the lower right convex hull of those figures and HALO sometimes can select rectangles that are arbitrarily distant from them.

4.2 Partitioning

In this part we are going to describe the geometrical properties and how the feasible set \mathcal{D} is partitioned. We will also highlight, how the derivatives around each partition are approximated adaptively during the iterations.

4.2.1 Division and Sampling

During the global search carried out by HALO, we use the same sampling and division criteria as in the DIRECT algorithm [18] because it demonstrated to be very robust and relatively easy to understand and implement the computer code.

Let's describe how the partitions \mathcal{D}_{i_k} are generated in the DIRECT algorithm. We define the vector $\mathbf{s}_{i_k} \in \mathbb{R}^N$ associated with the partition \mathcal{D}_{i_k} which measures the distance from its centroid to its boundary along all the coordinate directions (i.e. half the sides of the partition) at the iteration k , so that

$$\mathbf{s}_{i_k} = [|u_{i_k}^n - l_{i_k}^n| / 2]_{n=0}^N \quad (10)$$

We define the set of indices \mathcal{P}_{i_k} that contains the n th coordinate directions where the partition \mathcal{D}_{i_k} has its longest side,

$$\mathcal{P}_{i_k} = \{ n \in \mathbb{N} : s_{i_k}^{max} = \max\{s_{i_k}^n\}_{n=0}^N \} \quad (11)$$

successively, two points $\mathbf{x}_{i_k}^{p1}$ and $\mathbf{x}_{i_k}^{p2}$ are sampled for each coordinate axis parallel to the longest side of \mathcal{D}_{i_k} (namely along the p th coordinate)

$$\mathbf{x}_{i_k}^{p1} = \mathbf{x}_{i_k} + \Delta_{i_k} \mathbf{e}_p, \quad \mathbf{x}_{i_k}^{p2} = \mathbf{x}_{i_k} - \Delta_{i_k} \mathbf{e}_p, \quad \forall p \in \mathcal{P}_{i_k} \quad (12)$$

where \mathbf{e}_p is the p th orthonormal base of \mathbb{R}^N and the scalar Δ_{i_k} is given by two third the longest side of \mathcal{D}_{i_k}

$$\Delta_{i_k} = \frac{2}{3} s_{i_k}^{max} \quad (13)$$

From Eq. 12 we can see that two new points are generated along the coordinate of the longest side of the selected partition, such that the total number of new point generated per selected partition is $J = 2|\mathcal{P}_{i_k}|$.

Once the sampling inside a selected partition \mathcal{D}_{i_k} is performed, we start dividing it. In the DIRECT algorithm, the idea is to divide a partition into hypercubes and hyperrectangles such that the one that has the longest diagonal is always the partition with the lowest objective function value. We define the set \mathcal{T}_{i_k} which contains the minimum of the objective function value among the two new generated points $\mathbf{x}_{i_k}^{p1}$ and $\mathbf{x}_{i_k}^{p2}$ for each coordinate axis parallel to the longest side of \mathcal{D}_{i_k}

$$\mathcal{T}_{i_k} = \mathcal{T}_{i_k} \cup \{\min\{f(\mathbf{x}_{i_k}^{p1}), f(\mathbf{x}_{i_k}^{p2})\}\}, \quad \forall p \in \mathcal{P}_{i_k} \quad (14)$$

we start to divide \mathcal{D}_{i_k} in the order given by \mathcal{T}_{i_k} and perpendicular to the direction \mathbf{e}_p so that all the p th sides of \mathcal{D}_{i_k} are shrunken by half of Δ_{i_k} and consequently of a third the longest side of the partition \mathcal{D}_{i_k}

$$s_{i_k}^p = \frac{1}{2} \Delta_{i_k} = \frac{1}{3} s_{i_k}^{max}, \quad s_{i_k}^{p1} = s_{i_k}^{p2} = s_{i_k}^p \quad \forall p \in \mathcal{P}_{i_k} \quad (15)$$

and at the same time the sides $s_{i_k}^{p1}$ and $s_{i_k}^{p2}$ of two new partitions are also updated.

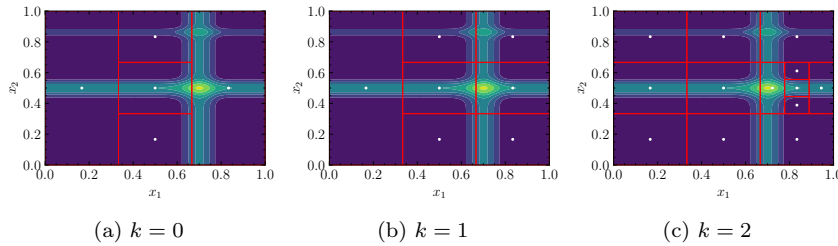


Fig. 2: A graphical representation of the division step.

4.2.2 Adaptive Gradients Approximation

After the sampling and the division processes are performed, the algorithm starts to collect information about the behavior of the objective function around every partition.

We define the set of the nearest neighbors of \mathcal{D}_{i_k} as follows

Definition 4.3 Given the partition \mathcal{D}_{i_k} and its centroid \mathbf{x}_{i_k} we define the nearest neighbors of \mathbf{x}_{i_k} the set of indices \mathcal{N}_{i_k} which contains the indices of the nearest point along the coordinate axis of \mathbb{R}^N .

We introduce a very simple property about where the nearest neighbors of a particular point \mathbf{x}_{i_k} are located if at iteration k the relative set \mathcal{D}_{i_k} is selected

Property 4.1 Given the representative point \mathbf{x}_{i_k} which is center of its relative partition \mathcal{D}_{i_k} . Then if for every iteration $k > \bar{k}$, the partition \mathcal{D}_{i_k} is selected, the nearest neighbours of \mathbf{x}_{i_k} are given by

$$\mathbf{x}_{i_k} \pm \Delta_{i_k} \mathbf{e}_n \in \mathcal{N}_{i_k}, \quad n = 1, \dots, N \quad (16)$$

where \mathbf{e}_n is the n th orthonormal basis of \mathbb{R}^N and \mathcal{N}_{i_k} the set of the nearest neighbours of \mathbf{x}_{i_k} .

Property 4.1 simply states that if we always select the partition \mathcal{D}_{i_k} at some iteration $k > \bar{k}$, the minimum distance $\Delta_{i_{\bar{k}}}$ from the nearest centroid of \mathbf{x}_{i_k} is obtained along all its Cartesian coordinates.

Given those assumptions, we could extract important information relative to each partition \mathcal{D}_{i_k} . The idea is to associate a vector to each partition \mathcal{D}_{i_k} which describes the intensity of variation of the objective function inside \mathcal{D}_{i_k} . Namely, we want to find an approximation of the gradient at each center of each partition by using only the points sampled so far by the algorithm.

If a partition is selected, the set of its nearest neighbors along the coordinate axis \mathcal{N}_{i_k} is given by the J points that it has generated through Eq. 12.

Now we can distinguish two cases depending if the selected partition is a hypercube or a hyperrectangle.

If the partition \mathcal{D}_{i_k} was an hypercube when it has been selected, then after sampling the new points, it has $J = 2|\mathcal{P}_{i_k}| = 2N$ nearest points along all the N coordinate axis at distance Δ_{i_k} . In this case the absolute slope at \mathbf{x}_{i_k} is computed using a central difference formula

$$|\tilde{\nabla} f(\mathbf{x}_{i_k})_n| = \frac{|f(\mathbf{x}_{i_k}^{p_1}) - f(\mathbf{x}_{i_k}^{p_2})|}{2\Delta_{i_k}}, \quad n = 1, \dots, N \quad (17)$$

Where the points $\mathbf{x}_{i_k}^{p_1}$ and $\mathbf{x}_{i_k}^{p_2}$ are given from Eq. 12, namely the two points generated from the centroid \mathbf{x}_{i_k} along the n th coordinate axis.

Similarly, we need also to compute the slopes for the new points $\mathbf{x}_{i_k}^j$, for every $j = 1, \dots, J$ that the partition \mathcal{D}_{i_k} has generated at iteration k . In this case, the approximation of the gradient associated with $\mathcal{D}_{i_k}^j$ is given by

$$|\tilde{\nabla} f(\mathbf{x}_{i_k}^j)_n| = \begin{cases} \frac{|f(\mathbf{x}_{i_k}^j) - f(\mathbf{x}_{i_k})|}{\Delta_{i_k}}, & \text{if } \mathbf{x}_{i_k} \in \mathcal{N}_{i_k}^j. \\ |\tilde{\nabla} f(\mathbf{x}_{i_k})_n|, & \text{otherwise.} \end{cases} \quad (18)$$

For the other $N - 1$ coordinates, the absolute slopes $|\tilde{\nabla} f(\mathbf{x}_{i_k}^j)_n|$ are set to the slope of the \mathbf{x}_{i_k} . This could lead to an incorrect estimation of the gradient associated at the partition $\mathcal{D}_{i_k}^j$. However, the effect will be negligible as the partition $\mathcal{D}_{i_k}^j$ will be selected and its gradient updated or when the size of the partition $\mathcal{D}_{i_k}^j$ is already relatively small.

In case \mathcal{D}_{i_k} was an hyperrectangle when it has been selected, then it has $J = 2|\mathcal{P}_{i_k}|$ nearest points along all the $|\mathcal{P}_{i_k}|$ coordinate axis at distance Δ_{i_k} , and a central difference

formula is used as before

$$|\tilde{\nabla} f(\mathbf{x}_{i_k})_n| = \begin{cases} \frac{|f(\mathbf{x}_{i_k}^{p_1}) - f(\mathbf{x}_{i_k}^{p_2})|}{2\Delta_{i_k}}, & \text{if } \mathbf{x}_{i_k}^{p_1}, \mathbf{x}_{i_k}^{p_2} \in \mathcal{N}_{i_k}. \\ |\tilde{\nabla} f(\mathbf{x}_{i_k})_n|, & \text{otherwise.} \end{cases} \quad (19)$$

For the remaining $N - |\mathcal{P}^{i_k}|$ coordinates we leave the slope unchanged in those directions.

As shown previously we also update the slopes for the points that \mathcal{D}_{i_k} has generated. In this case, the procedure is the same as in the case if the partition \mathcal{D}_{i_k} is a hypercube when selected.

The simple procedure described above tries to adaptively update the gradient at each selected centroid and at its neighbors only using the points sampled so far by the algorithm.

4.3 Coupling Strategy with Local Optimization Methods

In this work, we propose to couple our approach with local optimizers. This is motivated by the fact that the sampling scheme as described in section 4.2.1 despite its interesting properties, is not very convenient and efficient when the algorithm is approaching a stationary point. Indeed, the sampling scheme defined by the DIRECT algorithm makes sometimes the convergence of HALO towards a stationary point very slow. This possibly is due to the rigid structure of the sampling scheme since the algorithm is forced to sample along the coordinate directions with predefined constant step sizes of Δ_{i_k} as shown in Eq. 12, and no line-searches are employed to identify a more appropriate step size. We want to recall that, when a partition \mathcal{D}_{i_k} is selected the value of Δ_{i_k} is automatically given as $1/3$ the longest side of the hyperrectangle \mathcal{D}_{i_k} .

After those considerations, as soon as the slow convergence appears we abandon the sampling scheme defined by the DIRECT algorithm and start a local optimization routine. Here the goal is to use a local optimization routine only when a point \mathbf{x}_{i_k} is supposed to be in the neighborhood of a stationary point in order to do not over use it.

The coupling strategy is the following: if the index i_k satisfies Condition 1 or Condition 2 (or both of them) in Def. 4.2 and the partition \mathcal{D}_{i_k} has a half diagonal that is less than a scalar $\beta \in \mathbb{R}$ such that

$$\frac{\|\mathbf{u}_{i_k} - \mathbf{l}_{i_k}\|}{2} \leq \beta \quad (20)$$

then the relative centroid \mathbf{x}_{i_k} is considered as a starting point for the local optimizer.

To avoid starting the local optimizer in a similar location of the domain \mathcal{D} , we perform a simple nearest-neighbor search. More precisely before starting the local optimization from \mathbf{x}_{i_k} , we save in the set \mathcal{C}_k the indices j of all the points that are inside the ball with center \mathbf{x}_{i_k} (which is the starting point for the local optimizer) and radius r , by defining the set \mathcal{C}_k as follows

$$\mathcal{C}_k = \{j : \|\mathbf{x}_{i_k} - \mathbf{x}_{j_k}\| \leq r\}, \quad \forall j_k \in I_k, \quad i_k \neq j_k \quad (21)$$

then the local optimizer will start from \mathbf{x}_{i_k} and the set of indices updated with the index i_k

$$\mathcal{C}_k \cup i_k \quad (22)$$

Then if a new point \mathbf{x}_{p_k} satisfies Condition 1 or Condition 2 (or both of them) and the partition \mathcal{D}_{p_k} is such that Eq. 20 is satisfied then the local search starts from the point \mathbf{x}_{p_k} if and only if the following set is empty

$$\mathcal{B}_k = \{j : \|\mathbf{x}_{p_k} - \mathbf{x}_{j_k}\| \leq r\}, \quad \forall j_k \in C_k \quad (23)$$

which means that the point \mathbf{x}_{p_k} is not nearby to any of the neighbors already collected in the set C_k .

If the set \mathcal{B}_k is empty then we update the set C_k with respect to the neighbors of p_k

$$C_k = C_k \cup \{j : \|\mathbf{x}_{p_k} - \mathbf{x}_{j_k}\| \leq r\}, \quad \forall j_k \in I_k, \quad p_k \neq j_k \quad (24)$$

we start the local optimizer from \mathbf{x}_{p_k} and then update the set C_k with p_k .

Otherwise, if the set \mathcal{B}_k is not empty then the local search will not start from \mathbf{x}_{p_k} and as before we update the set C_k with p_k , namely

$$C_k \cup p_k \quad (25)$$

in this case, the set \mathcal{D}_{p_k} is not sampled nor divided. For this reason, the radius r should be fixed with respect to a relatively safe and low value to don't cancel out large portions of the domain, for example $r = 10^{-4}$.

4.4 Convergence and Stopping Criteria

In this paragraph, we will establish the convergence properties of HALO. Firstly, It is relevant to highlight the characteristic of the partitions $\{\mathcal{D}^{i_k} : i \in \mathcal{I}_k\}$ generated during the iterations k and the property of *strictly nested* sequences

Property 4.2 The sequence of partitions $\{\mathcal{D}^{i_k}\}$ is strictly nested if and only if

$$\bigcap_{k=0}^{+\infty} \mathcal{D}_{i_k} = \mathbf{x}_{i_k} \quad (26)$$

or equivalently that

$$\lim_{k \rightarrow +\infty} \|\mathbf{u}_{i_k} - \mathbf{l}_{i_k}\| = 0 \quad (27)$$

The Property 4.2 says that when any partition is continuously selected and divided at infinity the partition itself it'll 'collapse' to a point. As shown in [13] all the sequence of points generated by the algorithm should be dense on \mathcal{D} to converge to a global minimum.

The following proposition shows that the so-called everywhere dense property of HALO is simply achieved if one of the largest partitions is always selected

Proposition 4.1 *Given Property 4.2, if for every iteration k the largest partitions \mathcal{D}_{i_k} is always selected such that $i_k \in \mathcal{I}_k^{max}$, then for $k \rightarrow \infty$ and for every $\tilde{\mathbf{x}} \in \mathcal{D}$, the sequence of sets $\{\mathcal{D}_{i_k}\}$ are dense such that*

$$\bigcap_{k=0}^{\infty} \mathcal{D}_{i_k} = \{\tilde{\mathbf{x}}\} \quad \forall i_k \in \mathcal{I}_k \quad (28)$$

Proof The proof follows simply from the fact that the following identity is valid for every i_k

$$\lim_{k \rightarrow +\infty} \|\mathbf{u}_{i_k} - \mathbf{l}_{i_k}\| \leq \|\mathbf{u}_{j_k} - \mathbf{l}_{j_k}\| = 0 \quad (29)$$

with $j_k \in \mathcal{I}_k^{max}$, with $\mathcal{I}_k^{max} = \{i_k \in I_k : \|\mathbf{u}_{i_k} - \mathbf{l}_{i_k}\| = \max_{i_k \in \mathcal{I}_k} \|\mathbf{u}_{i_k} - \mathbf{l}_{i_k}\|\}$.

Therefore, if the algorithm produces dense sets across all the domain \mathcal{D} , then for k sufficiently large the algorithm will converge also at the global minimum of f .

In general, if on one side is not difficult to design an algorithm that satisfies the everywhere dense property on the other we would prefer an algorithm that produces dense only around the global minimizers and not all across the domain \mathcal{D} . This, unfortunately, is very difficult to achieve in practice. This is generally possible to obtain if one has prior knowledge of the global Lipschitz constant [42].

For this reason, the stopping criterion for the HALO is based mainly on the maximum number of function evaluations, which is also one of the most used criteria in engineering applications.

In HALO, we can show that the exact value of the global Lipschitz constant is obtained again when the algorithm iterates indefinitely to infinity. First, we can highlight an important characteristic of the distance Δ_{i_k} in the next proposition

Proposition 4.2 *Given the center \mathbf{x}_{i_k} of its relative partition \mathcal{D}_{i_k} . If the algorithm satisfies Property 4.2 and Property 4.1 then the distance Δ_{i_k} from the nearest point of \mathbf{x}_{i_k} satisfies the following limit*

$$\lim_{k \rightarrow +\infty} \Delta_{i_k} = 0 \quad (30)$$

Proof If Property 4.2 holds the algorithm produces at least one sequence of strictly nested partitions $\{\mathcal{D}^{i_k}\}$ such that

$$\lim_{k \rightarrow +\infty} \mathbf{u}_{i_k} = \mathbf{x}_{i_k}, \quad \lim_{k \rightarrow +\infty} \mathbf{l}_{i_k} = \mathbf{x}_{i_k}, \quad \lim_{k \rightarrow +\infty} \|\mathbf{u}_{i_k} - \mathbf{l}_{i_k}\| = 0 \quad (31)$$

then we know that if the partition \mathcal{D}_{i_k} is selected, then exactly $J = 2|\mathcal{P}_{i_k}|$ (see Eq. 11) points are sampled inside \mathcal{D}_{i_k} . Consequently, for every $j = 1, \dots, J$ we have that

$$\Delta_{i_k} = \|\mathbf{x}_{i_k} - \mathbf{x}_{i_k}^j\| \leq \|\mathbf{l}_{i_k} - \mathbf{x}_{i_k}\| \leq \|\mathbf{u}_{i_k} - \mathbf{l}_{i_k}\| \quad (32)$$

considering Eq. 31 it follows that $\lim_{k \rightarrow +\infty} \Delta_{i_k} = 0$

The Proposition 4.2 says that the minimum distance Δ_{i_k} from the nearest neighbors of \mathbf{x}_{i_k} tends to zero as the iteration of the algorithm k goes to infinity and as the relative partition \mathcal{D}_{i_k} is continuously selected. As a partition \mathcal{D}_{i_k} is selected during the iterations, the information contained in its gradient becomes more precise, so that we can introduce the following proposition

Proposition 4.3 *Given the representative point \mathbf{x}_{i_k} which is center of its relative partition \mathcal{D}_{i_k} . If HALO satisfies has Property 4.2 and Property 4.1 and its sampling scheme satisfies Property 4.1 then the gradient associated to the partition \mathcal{D}_{i_k} converge to the true gradient at \mathbf{x}_{i_k}*

$$\lim_{k \rightarrow +\infty} \tilde{\nabla} f(\mathbf{x}_{i_k}) = \nabla f(\mathbf{x}_{i_k}) \quad (33)$$

Proof If Property 4.1 is satisfied then there exist k such that for every $\bar{k} > k$ the centroid \mathbf{x}^{i_k} has its nearest point along all the coordinate directions. Then using the results from Property 4.2 and for the definition of derivative it follows that $\lim_{k \rightarrow +\infty} \tilde{\nabla} f(\mathbf{x}^{i_k}) = \nabla f(\mathbf{x}^{i_k})$

In Proposition 4.3 we showed that as the partition \mathcal{D}_{i_k} becomes dense and it starts to collapse into its centroid \mathbf{x}^{i_k} , the associated gradient $\tilde{\nabla} f(\mathbf{x}^{i_k})$ becomes a more precise approximation of the true gradient $\nabla f(\mathbf{x}^{i_k})$.

Since HALO satisfies the Prop. 4.1, we can obtain the exact value of the gradient at any point of the domain \mathcal{D} . Consequently, also the global Lipschitz constant

Proposition 4.4 *If HALO satisfies Proposition 4.3 then*

$$\lim_{k \rightarrow \infty} \max_{i_k \in \mathcal{I}_k} \{ \|\tilde{\nabla} f(\mathbf{x}_{i_k})\| \} = L \quad (34)$$

Proof The proof is given directly by using the results of Proposition 4.3 and applying it for every $i_k \in \mathcal{I}_k$ and taking the maximum.

4.5 A Detailed Implementation of HALO

The simplified pseudocode of HALO is given in Alg. 2. In the following, we will describe some of the main passages of the pseudocode.

The core part of HALO is inside the function `Main` whereas input it receives the criterion to terminate the algorithm, based on the maximum number of function evaluations or by the maximum number of iterations. The user gives as input also the box constraints of the optimization problem \mathcal{D} .

Fixing the counter k to zero, at line 8 and 9 we define the indices of the selected partitions \mathcal{I}_k^* , and the matrix $\mathbf{S} \in \mathbb{R}^{|\mathcal{I}_k^*| \times N}$ where at each entry contains the vector \mathbf{s} defined in Eq. 10.

In line 10, we start a for loop with respect to the indices of each selected partition and it is mainly devoted to the computation of $\Delta_{i_k^*}$ as described in Section 4.2.1.

In line 17, another for loop starts cycling with respect to each element of the set $\mathcal{P}_{i_k^*}$, as defined in line 13 and in Eq. 11. This is the loop where the sampling is performed and shown in section 4.2.1. We also start to compute the slopes, by updating in the matrix $\mathbf{G} \in \mathbb{R}^{|\mathcal{I}_k^*| \times N}$ which collects the estimation of the gradients as described in section 4.2.2. The notation $\mathbf{G}_{i_k^*, p}$ means that the coordinate p of the gradient relative of the i_k^* th partition is updated.

After this inner for loop, in line 28 we perform a sorting of the indices of the set $\mathcal{T}_{i_k^*}$ defined in Eq. 14 and at line 30, we can call the function (line 67) which performs the division of the set $\mathcal{D}_{i_k^*}$.

Once the outer loop defined in line 11 is completed, given the information contained in the matrix \mathbf{G} , we call the function that has the task to compute the values of the local Lipschitz constants collected in the vector $\mathbf{l} \in \mathbb{R}^{|\mathcal{I}_k^*|}$. On lines 32 and 33, we define the vectors $\mathbf{v} \in \mathbb{R}^{|\mathcal{I}_k^*|}$ and $\mathbf{h} \in \mathbb{R}^{|\mathcal{I}_k^*|}$ that contain the half of the distances from the center of each j th partition to its vertices and the norm of the estimation of each gradient (namely the norm of each row of \mathbf{G}). In line 35, we compute (in a vectorized form) the estimation of the local Lipschitz constant is computed according to Eq. 6.

The next task, is using the local Lipschitz constants collected in the vector \mathbf{l} to compute the lower bounds and select, based on Def. 4.2 the most promising partitions.

The value of the lower bounds is contained in the vector $\mathbf{r} \in \mathbb{R}^{|\mathcal{I}_k^*|}$. The indices q_1^* , q_2^* and q_3^* represent the index of the partition with minimum lower bound, the partition with the minimum objective function value, and the partition that among the ones with the largest diagonal is the one that has the minimum lower bound. Can happen that one index satisfies more than one condition (e.g. $q_1^* = q_2^*$) so that one should care about to do not allow duplicates in the set \mathcal{I}_k^* .

On lines 43 and 48, we evaluate if a local search has been already performed from the centroid of that partition and if they satisfy Eq. 20. If those two conditions are met, the local search will start, as explained in section 4.3. Note that the largest hyperrectangle q_3^* will be always selected. In the end, the set of the selected partitions is returned (and also duplicates are removed) and a new loop with respect to its elements can start.

We conclude this section, showing in Fig. 3 the behavior of HALO for a simple one-dimensional function. The red dots represent the centroids of each partition, the blue line highlights the value of the local Lipschitz constant in its slope and the yellow dots emphasize the value of the lower bounds at the boundary of each partition.

At iteration $k = 0$ is possible to notice that, the value of Lipschitz constants with respect to the three partitions does not reflect the underlying trend of the objective function, because those three points have a similar objective function value and there is a relatively large distance between them.

At iteration $k = 1$, the partition \mathcal{D}_0 is the only selected and divided because it satisfies Condition 1, Condition 2 and Condition 3. It is also possible to notice that the values of the lower bounds are already much more precise.

At iteration $k = 2$, two intervals are selected and divided: \mathcal{D}_0 that satisfies Condition 2 (has the lowest function value) and \mathcal{D}_1 that satisfies Condition 1 and Condition 3 (it has the overall lowest lower-bound and it is the largest partition with the lowest lower bound).

Finally at iteration $k = 3$, the following two intervals are divided: \mathcal{D}_2 that satisfies Condition 3 and \mathcal{D}_7 that satisfies Condition 1 and Condition 2. This last Fig. 3d, enables us to observe that all the values of the lower bounds are now quite precise, and this process is completely automatic in HALO and no crucial hyper-parameters are needed to be settled by the user.

5 Numerical Results

In this section, we will test the performance of HALO to other GO algorithms considering a large collection of test functions divided into three different benchmarks. We also provide a parametric study for the parameter β defined in Eq. 20 to understand if it's possible to give a general recommendation for the user about its value. Most of the codes (algorithms and test functions) used in this work are freely available at the following repository at this link <https://github.com/dannyzx/HALO>.

5.1 Experimental Set-up

In the next paragraphs, we will present all the algorithms, the test functions, and the stopping criteria used in this numerical campaign.

5.1.1 Algorithms

The algorithms considered in the numerical experiments are the following:

1. HALO_{L-BFGS-B} and HALO_{SDBOX}: are the two versions of HALO coupled with two different local optimizers, namely a quasi-Newton method for bound constrained problems (L-BFGS-B) [37] and a derivative-free coordinate descent method with an Armijo-type linesearch for bound constrained optimization [38] (SD-BOX). In both versions of HALO, there is only one hyperparameter to set which is β as defined in Eq. 20. The parameter β in Eq. 20 controls how small a selected partition has to be before the local search can be started from its centroid. For the current experiment we fixed $\beta = 10^{-4}$. In HALO_{L-BFGS-B}, the gradients inside the Quasi-Newton code are computed through finite difference methods.
2. HLO: it is HALO_{SDBOX} but without the adaptive estimates of the local Lipschitz constants given in the formula 6. Instead, the calculations of the lower bounds are based on the value of the estimate of the global Lipschitz constant only, namely all local Lipschitz constants are fixed as follows

$$\tilde{L}_{i_k} = \max_{i_k \in \mathcal{I}_k} \|\tilde{\nabla} f(\mathbf{x}_{i_k})\| \quad (35)$$

In this way, we can understand if an estimation of the local Lipschitz constants accelerates the convergence respect using an estimate of the global Lipschitz constant.

3. DIRECT [18]: the classical DIRECT algorithm with the only hyperparameter ϵ fixed $10^{-4}|f_{min}|$ as in [18].
4. DIRMIN [36]: an efficient hybridization of the DIRECT algorithm, where local optimizations are started from each of the potentially optimal hyperrectangles of DIRECT. Here we use the same derivative-free local optimizer as in HALO_{SDBOX} namely the algorithm defined in [38]. DIRMIN demonstrated to accelerate the convergence of DIRECT in many test functions as shown in [36]. Furthermore, it proved to be the best performing global optimization algorithm in a real-world application involving a hull form shape optimization problem, among other derivative-free hybrid GO algorithms [43].
5. CMA-ES [5]: it is one of the most popular stochastic meta-heuristic approaches and showed good performance in many applications. It is also one of the most competitive among the algorithm of this kind [44].

The hyperparameter σ_0 is fixed to 1/4 of the domain as suggested by the author. Because of the stochastic nature of the algorithm, we run 50 different experiments for every test function.

Algorithm 2: Hybrid Adaptive Lipschitzian Optimization (HALO)

```

1 function Main(MaxIter, MaxFunEval, D)
2   k ← 0
3   Ck, G, S ← 0, [], []
4   for k to MaxIter do
5     if k > 0 then
6       l ← compute_Lipschitz(G, S)
7       Tk ← Select(Tk, l, Ck)
8     else
9       Tk ← {0}
10      Sk ← [un - ln/2]Nn=1
11      for ik* in Tk do
12        sik* ← Sik*
13        skmax ← max{sik*}
14        Pik* ← arg max{sik*}
15        Δik* ←  $\frac{2}{3}$  skmax
16        j ← 0
17        Vik* ← ∅
18        for p in Pik* do
19          xkp1 ← xik* + Δik* ep
20          f(xkp1) ← Fun_Eval(xkp1)
21          fik*+1 ← f(xkp1)
22          Gik*+1,p ← |f(xkp1) - f(xik*)|/Δik*
23          xkp2 ← xik* - Δik* ep
24          f(xkp2) ← Fun_Eval(xkp2)
25          fik*+2 ← f(xkp2)
26          Gik*+2,p ← |f(xkp2) - f(xik*)|/Δik*
27          Gik*,p ← |f(xkp1) - f(xkp2)|/2Δik*
28          Tik* ← Tik* ∪ {min{f(xkp1), f(xkp2)}}
29        Uik* ← argsort{Tik*}
30        Tk ← Partitioning(Uik*, S, V)
31 function Compute_Lipschitz(G)
32   v ← (||Sj||)1 ≤ j ≤ |Ik|}
33   h ← (||Gj||)1 ≤ j ≤ |Ik|}
34   α ← v/√N
35   l ← α ⊙ h + (1 - α) ⊙ max{h}
36   return l
37 function Selection(Tk, Ck)
38   r ← f - v ⊙ 1
39   q1* ← arg min{r}
40   q2* ← arg min{f}
41   Q3 ← arg max{v}
42   q3* ← arg minq3 ∈ Q3 {1}
43   if q1* ∉ Ck and vq1* ≤ β then
44     x0 ← xq1*
45     Local_Search(xq1*, Ck)
46   else
47     Tk ← Tk ∪ {q1*}
48   if q2* ∉ Ck and vq2* ≤ β then
49     x0 ← xq2*
50     Local_Search(xq2*, Ck)
51   else
52     Tk ← Tk ∪ {q2*}
53   Tk ← Tk ∪ {q3*}
54   return Tk
55 function Local_Search(x0, Ck)
56   xpk ← x0
57   if Ck = ∅ then
58     Ck ← {j ∈ Ik : ||xpk - xjk|| ≤ r}
59     x ← Local_Optimizer(xpk)
60     return x
61   else
62     Bk ← {j ∈ Ck : ||xpk - xjk|| ≤ r}
63     if Bk ≠ ∅ then
64       Ck ← Ck ∪ {j ∈ Ik : ||xpk - xjk|| ≤ r}
65       x ← Local_Optimizer(xpk)
66       return x
67     else
68       Ck ← Ck ∪ pk
69 function Partitioning(Uik*, Pik*, S, V)
70   for u in Uik* do
71     m ← Pik*,u
72     Sik*,m ← Δ/2
73     Sik*+1 ← Sik*
74     Sik*+2 ← Sik*
75     Tk ← Tk ∪ {|Ik| + 1, |Ik| + 2}
76   return Tk

```

5.1.2 Test Functions

We tested all the described algorithms using three different benchmarks:

1. The first benchmark is built by a function generator defined in [40]. In this case we considered 100 test functions for every dimension $N \in \{2, 3, 4, 6, 8, 10\}$, namely we generated 600 different test functions.

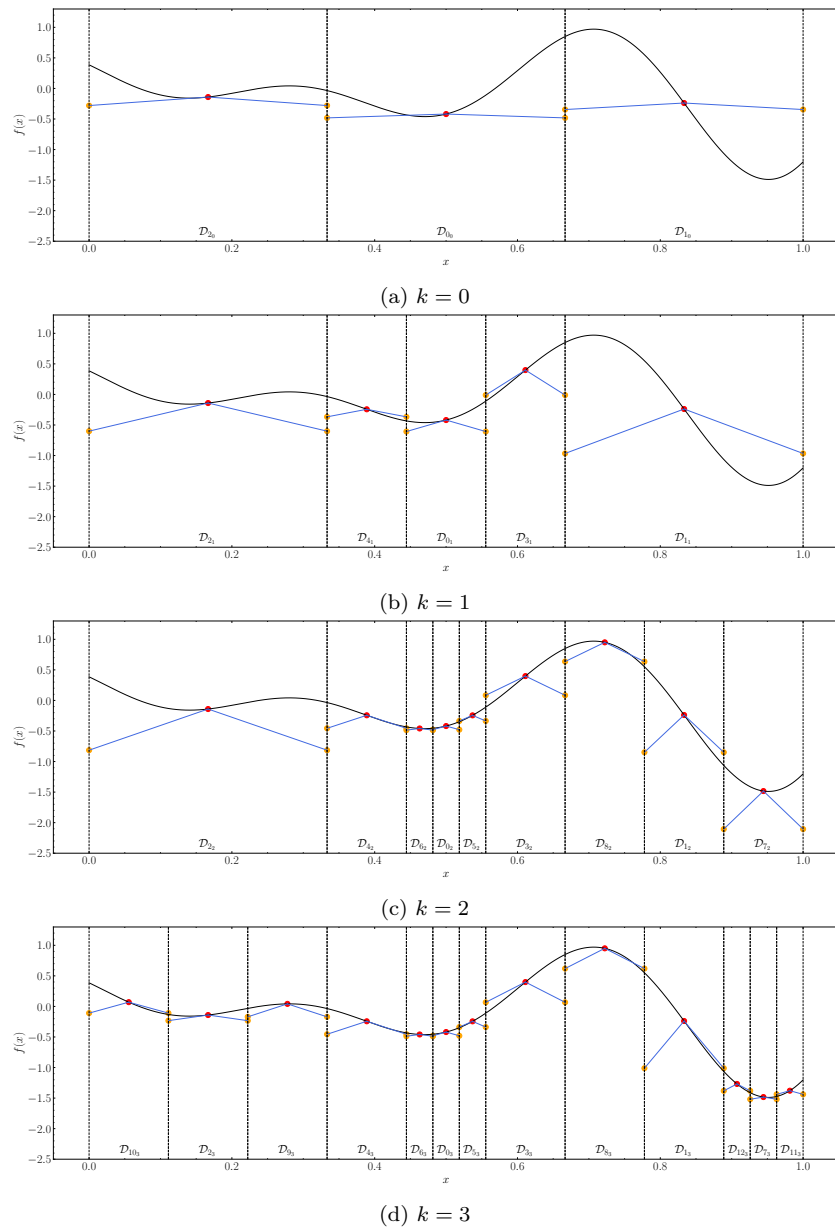


Fig. 3: An example of HALO for a one-dimensional function.

There are two hyperparameters that we need to set for the function generator: the number of stationary points and their smoothness. In this experiment, the number of stationary points S are uniformly sampled with $S \in \{1, \dots, 100\}$ and the smoothing parameter uniformly chosen in $[2, 3]$ as in [45].

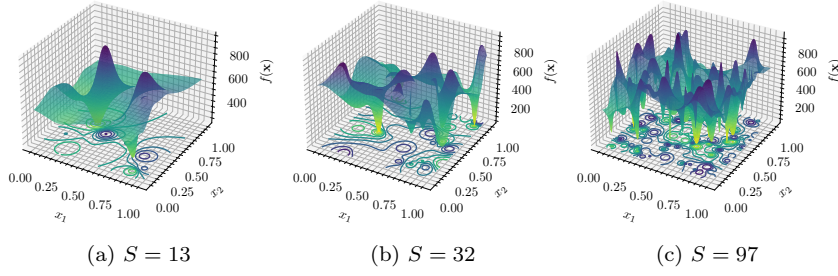


Fig. 4: Example of the first benchmark considered, S represents the number of stationary points.

- The second benchmark is composed of objective functions generated from the methodology described in [41]. The original implementation is written C programming language. We rewrote the software in Python programming language.

As in the previous benchmark, 100 test functions are considered for every $N \in \{2, 3, 4, 6, 8, 10\}$, and 600 different test are generated.

Here there are various hyperparameters to set: the distance A from the global minimizer to the vertex of the paraboloid, the size of the basin of attraction B of the global minimizer, and the number of local minima C .

To produce somehow a challenging benchmark, one should choose a global minimizer to be far from the vertex of the paraboloid and at the same time by fixing a basin of attraction very small. To achieve that, we fixed $A \in [0.8, 1)$, $B \in [0.1, 0.2)$ and $C \in \{3, 10\}$, all uniformly at random.

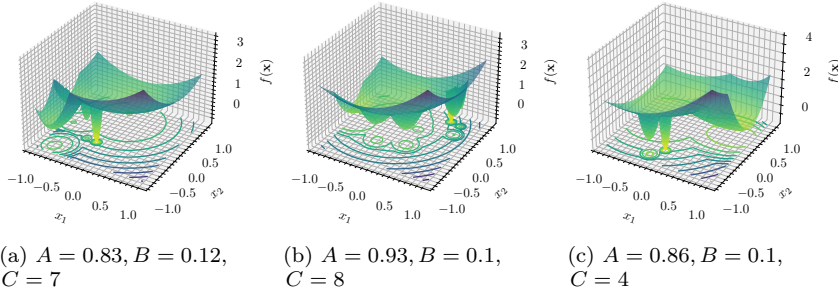


Fig. 5: Example of the second benchmark considered, A is the distance from the global minimizer to the vertex of the paraboloid, B the radius of the basin of attraction of the global minimizer and C the number of local minima.

- The last benchmark is composed of popular test functions used many times to evaluate the performance of both local/global optimization algorithms like the Rosenbrock, Beale, Michalewicz, Hartmann as defined in [46]. A total of different 191 functions are considered.

When a particular test function is generalizable for any dimension N , then the same test function is considered for different $N \in \{2, 3, 4, 6, 8, 10\}$, so that the total number of experiments using this benchmark is 496.

Finally, when a function has the global minimum at the center of its domain, the global minimizer is randomly shifted inside the domain.

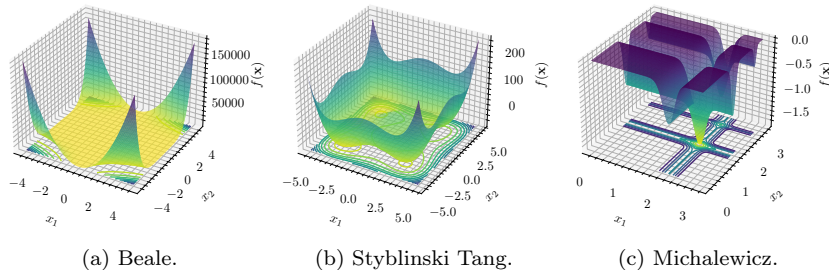


Fig. 6: Example of the third benchmark considered.

5.1.3 Stopping Criteria

The termination criteria are reached when the relative error to the global optimal objective function value f_{glob} is such that

$$\frac{f - f_{\text{glob}}}{|f_{\text{glob}}|} \leq 10^{-4} \quad (36)$$

The second termination criteria are based on the maximum number of function evaluations which in this work are fixed to 10000 independently of the dimensionality of the problem. This means that if an algorithm exceeds 10000 function evaluations without meeting the criterion given in Eq. 36 then the run it's considered failed.

5.2 Comparison Results and Discussion

In the next three subsections, we will show and discuss the numerical results obtained by each algorithm for every benchmark considered in this work.

Due to a large number of objective functions considered for each benchmark, we will mainly summarize the results in operational characteristics [47] (also known as performance profiles [48]) and tables.

5.2.1 First Benchmark Results

In Tab. 1 we summarized the numerical results obtained in the first benchmark.

The best performing algorithm is also in this case HALO_L-BFGS-B both in terms of the percentage of problems solved and in terms of the number of functions evaluations while the CMA-ES algorithm seemed to be the worst performing one.

In this benchmark, there is not a remarkable difference in performance between the two versions of HALO equipped with the two different local optimizers.

What we think is interesting is the difference in performance between HALO_{SDBOX} and HLO. HALO_{SDBOX} solves 14.2% more problems than HLO and also in a much faster way by looking at the operational characteristic of this benchmark in Fig.7a. HLO is also performs worse than DIRECT. We tried to analyze why this lack of performance in HLO is occurring in this case. From our analysis, in many objective functions happen that by using only the estimate of the global Lipschitz constant made the algorithm HLO select only two hyperrectangles: the one with minimum objective function value (which is selected apriori) and the hyperrectangle that is among the ones with the largest diagonal has the lowest value of the objective function. Consequently, if the global minimum is not located in one of those two partitions, the overall convergence of the algorithm is somehow compromised.

In this benchmark, DIRMIN greatly accelerates the convergence of DIRECT. But what is interesting the most is to look at the performance of DIRMIN varying the dimensionality of the problem as shown in Fig. 8a. We can notice that for $N \geq 6$ DIRMIN performs better than DIRECT and for $N \geq 8$ better than all the algorithms considered in this benchmark, highlighting that DIRMIN seems to be more insensitive to the curse of the dimensionality; possibly because DIRMIN makes strong usage of the local optimization algorithm which is a good way to catch the local trend of the objective function.

We end our discussion by noticing that CMA-ES gets stuck in bad local minima for the majority of the objective functions, and independently of the dimensionality of the problem (see Fig. 8a). For the CMA-ES, in Tab. 1 is reported the average of the percentage of solved problems with the standard deviation inside parenthesis.

Table 1: Resume of the numerical results for the first benchmark.

Numerical results		
Algorithm	Percentage solved	Average functions evaluations
HALO _{L-BFGS-B}	74.1	1605.5
HALO _{SDBOX}	73.3	1655.3
HLO	59.1	1725.1
DIRMIN	69.5	1751.6
DIRECT	63.0	1762.8
CMA-ES	22.3 (1.3)	354.0

5.2.2 Second Benchmark Results

In Tab. 2 we summarized the numerical results obtained in the second and last benchmark.

In this case, we have the best performing algorithm is HALO_{SD-BOX} because solves most of the problems but the performance is somehow really similar to HALO_{L-BFGS-B} while the CMA-ES algorithm also in this benchmark is the worst performing one.

From our analysis, this highly challenging benchmark tests the capability of a GO algorithm to explore efficiently the entire domain. An algorithm that puts too much weight on exploitation rather than exploration could fail miserably in many of the test

functions considered in this benchmark. This is because the basin of attraction of the global minimum is very small and the distance from the vertex of the paraboloid (which acts as a 'trap') to the global minimizer is fixed relatively high in all the test functions considered.

It's interesting also in this case to analyze the difference between using the local Lipschitz constant as in HALO_{SDBOX} or the global one like in HLO. Also, this last benchmark confirms that using an estimate of the local Lipschitz constant for each partition produces better performance since HALO_{SDBOX} solves 3.2% more problems than HLO.

Analyzing the performance of DIRECT again its hybrid counterpart DIRMIN we can see that the latter is much less effective than DIRECT simply because too many local searches have started and ended up at the vertex of the paraboloid.

Finally, it seems that CMA-ES has strong difficulty in solving any of the objective functions since from our results almost 100% of the time it got stuck at the paraboloid vertex.

Table 2: Resume of the numerical results for the second benchmark.

Numerical results		
Algorithm	Percentage solved	Average functions evaluations
HALO _{L-BFGS-B}	40.5	1877.5
HALO _{SDBOX}	40.8	1999.8
HLO	37.6	1946.8
DIRMIN	19.3	3392.5
DIRECT	31.6	1835.5
CMA-ES	10^{-3} (10^{-3})	10000

5.2.3 Third Benchmark Results

In Tab. 3 we summarized the numerical results obtained in the last and third benchmark.

The best performing algorithm is HALO_{L-BFGS-B} both in terms of the percentage of problems solved and in terms of the number of function evaluations. On the other side, the DIRECT algorithm seemed to be the relatively worst performing one.

In this benchmark, there is some noticeable difference in performance between the two versions of HALO with the two different local optimizers. The one equipped with the gradient based optimizer HALO_{L-BFGS-B} is more efficient than HALO_{SDBOX} because on average solved 2% more problems with 100 functions evaluation less. Between HALO_{SDBOX} and HLO there is not a big difference in terms of the number of problems solved but there is a difference in performances because HALO_{SDBOX} solves the problems with 200 function evaluations less than HLO on average. This confirms that in this benchmark, an estimate of the local Lipschitz constant accelerates the algorithm toward the global minimizers in a faster way with respect to using only an estimate of the global Lipschitz constant. This can be noticed from the operational characteristic in Fig. 7c.

While DIRMIN greatly accelerates the convergence of DIRECT does not perform better than HALO and HLO. This is possibly, because DIRECT-type approaches based on the concept of potentially optimal hyperrectangles usually sample a large number of

them, with the possibility to spend many functions evaluations in exploring sub-optimal regions of the domain \mathcal{D} .

The CMA-ES seems also to achieve better performance with respect to the DIRECT algorithm but less with respect to the rest of the other approaches considered.

In Fig. 8c we highlighted the performances of all the algorithms varying the dimensionality N . It can be noticed that: HALO_{L-BFGS-B}, HALO_{SDBOX}, HLO and DIRMIN have similar performances varying the dimensionality, CMA-ES also similar but under-performing for dimensionality $N = 2$, but competitive for the remaining values of N . Instead DIRECT, shows in this benchmark a marked deterioration in performance for $N \geq 6$.

Table 3: Resume of the numerical results for the third benchmark.

Numerical results		
Algorithm	Percentage solved	Average functions evaluations
HALO _{L-BFGS-B}	72.9	776.8
HALO _{SDBOX}	70.1	842.2
HLO	69.1	1015.6
DIRMIN	67.1	965.7
DIRECT	61.2	1315.9
CMA-ES	65.2 (1.0)	898.9

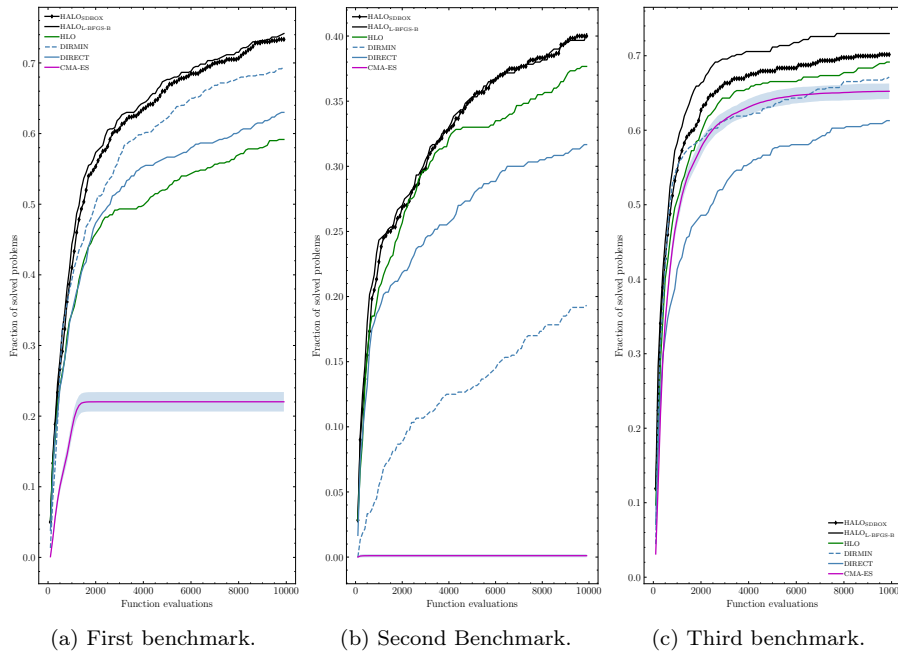
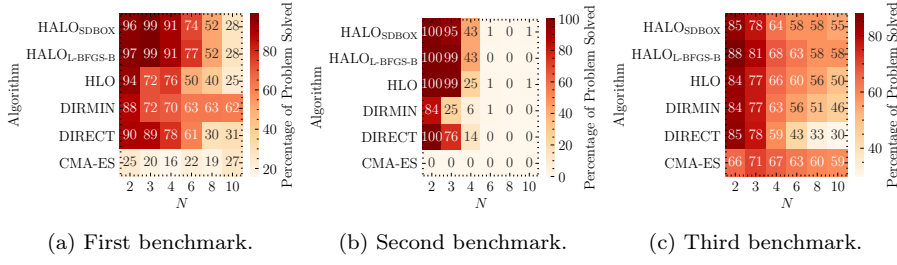
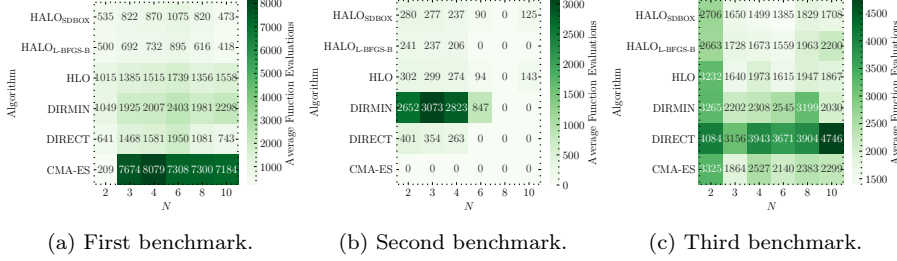


Fig. 7: Operational characteristics for the three benchmarks.

Fig. 8: Percentage of problem solved varying the dimensionality N .Fig. 9: Average number of functions evaluations varying the dimensionality N .

5.2.4 Sensitivity Analysis with Respect to the Parameter β

In this section, we will discuss and show the effect of various choices of the parameter β to the performance of HALO. Let's remind the reader that the β parameter is used in the Eq. 20 to check if a partition \mathcal{D}_{i_k} is small enough to consider its centroid as starting point for the local optimizer.

A value of β very small will make HALO to use the local optimizer rarely, while an higher value will force HALO to use the local optimizer more frequently.

However, the user should be careful in selecting an high value of β because once the local search starts from the centroid of the partition, the latter will never be partitioned in the future.

We run HALO_{L-BFGS-B} and HALO_{SDBOX} with values of β in

$$\beta \in \{10^{-1}, 10^{-2}, 10^{-3}, 10^{-4}, 10^{-5}, 10^{-6}\} \quad (37)$$

and for all the functions contained in the three different benchmarks. The result, are summarized in Tab. 4. In general, seems that the performance of HALO is quite robust with respect to the choice of the parameter β , especially for the choice of $\beta \in [10^{-2}, 10^{-6}]$ as it is possible to notice also from the operational characteristics in Fig. 10a and in Fig. 10b for HALO_{L-BFGS-B} and HALO_{SDBOX} respectively.

Always for $\beta \in [10^{-2}, 10^{-6}]$, it seems that HALO is also robust to the choice of the local optimizer because there is not a very noticeable difference in performance between HALO_{SDBOX} and HALO_{L-BFGS-B}, even if the latter showed to be the best performing both in terms of average function evaluations and percentage of problems solved.

In Tab. 4, is also reported on average, how many local optimization routines start for each optimization problem. On average, one and two local optimization routines have

Table 4: Resume of the numerical results for the sensitivity analysis with respect to the parameter β .

β	Numerical results					
	Percentage solved		Average functions evaluations		Average n° local searches	
	HALO _{L-BFGS-B}	HALO _{SDBOX}	HALO _{L-BFGS-B}	HALO _{SDBOX}	HALO _{L-BFGS-B}	HALO _{SDBOX}
10^{-1}	60.0	60.0	1303.2 (2038.6)	1600.3 (2249.4)	3.6 (6.3)	3.4 (6.1)
10^{-2}	61.3	60.6	1310.8 (1939.5)	1493.7 (2042.4)	1.9 (2.4)	1.8 (2.4)
10^{-3}	61.4	60.2	1332.3 (1957.9)	1469.2 (2053.0)	1.3 (0.9)	1.3 (0.9)
10^{-4}	61.7	60.7	1394.3 (2034.7)	1442.5 (2005.6)	1.0 (0.8)	1.0 (0.8)
10^{-5}	61.3	60.7	1411.0 (2025.5)	1484.3 (2061.5)	1.0 (0.8)	0.9 (0.8)
10^{-6}	61.3	60.7	1414.5 (1995.7)	1524.4 (2102.5)	0.9 (0.8)	0.9 (0.8)

started respectively for $\beta \in [10^{-3}, 10^{-6}]$ and when $\beta = 10^{-2}$, for both HALO_{SDBOX} and HALO_{L-BFGS-B}.

In general, the situation changes when $\beta = 10^{-1}$ where both HALO_{SDBOX} and HALO_{L-BFGS-B} lose some performance especially for dimension $N = 3$ (see Fig. 11). Finally based on the results our recommendation for the value of β are the following:

- do not choose a value of β less than 10^{-4} so that HALO will not spend too much functions evaluations on very small hyperrectangles and also to avoid eventual numerical instabilities.
- if the objective function is supposed to contain noise we recommend to use the derivative-free version of HALO namely HALO_{SDBOX} with $\beta \in [10^{-2}, 10^{-4}]$. Otherwise, HALO_{L-BFGS-B} should be the default choice always with $\beta \in [10^{-2}, 10^{-4}]$.

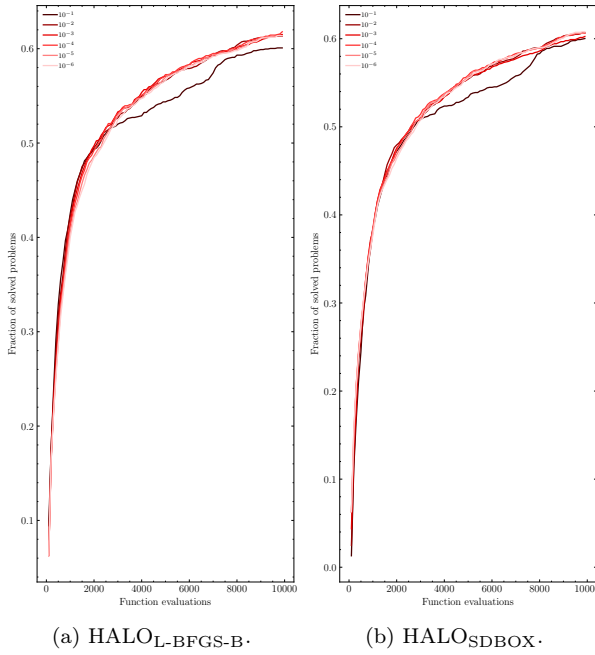


Fig. 10: Operational characteristics for the two versions of HALO.

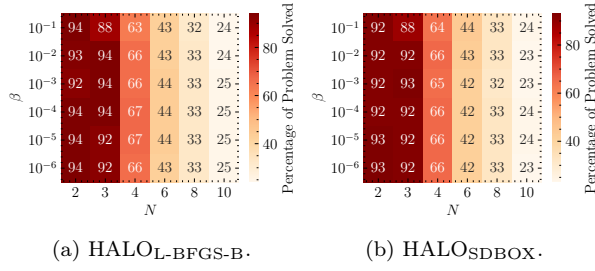


Fig. 11: Percentage of problems solved varying the dimensionality N .

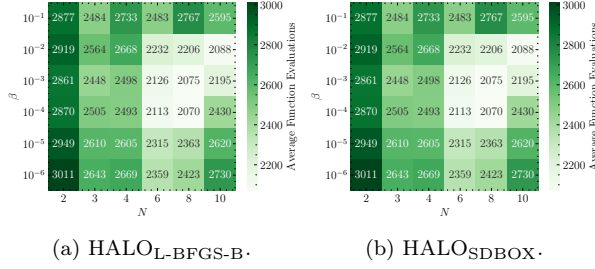


Fig. 12: Average number of functions evaluations varying the dimensionality N .

6 Conclusions

In this work, we provided a deterministic partition-based Global Optimization algorithm HALO (Hybrid Adaptive Lipschitzian Optimization) with an adaptive procedure to estimate the local Lipschitz constant associated with each partition or sub-region \mathcal{D}_i of the box domain \mathcal{D} .

The estimate is automatically determined based on the size of the partition \mathcal{D}_i so that no crucial hyper-parameters must be defined apriori by the user, by balancing the information between the current estimate of the global Lipschitz constant and the approximation of the gradient associated to the centroids of each partition.

We showed and motivate a simple coupling strategy with local optimization algorithms to accelerate the convergence speed towards a stationary point.

In the end, we compared the performance of HALO to popular GO algorithms using three different benchmarks containing hundreds of test functions. We also provided a sensitivity analysis regarding the hyperparameter which controls the local searches. The numerical results suggest that the performance of HALO is quite robust to that hyperparameter.

Finally, HALO showed to be strongly competitive and could definitively be considered as an additional tool for solving complex real-world GO problems.

References

1. Wyn L. Price. A controlled random search procedure for global optimisation. *The Computer Journal*, 20(4):367–370, 1977.
2. Lawrence Davis. *Handbook of genetic algorithms*. CumInCAD, 1991.
3. David S Johnson, Cecilia R Aragon, Lyle A McGeoch, and Catherine Schevon. Optimization by simulated annealing: An experimental evaluation; part i, graph partitioning. *Operations research*, 37(6):865–892, 1989.
4. James Kennedy and Russell Eberhart. Particle swarm optimization. In *Proceedings of ICNN'95-International Conference on Neural Networks*, volume 4, pages 1942–1948. IEEE, 1995.
5. Nikolaus Hansen and Andreas Ostermeier. Completely derandomized self-adaptation in evolution strategies. *Evolutionary computation*, 9(2):159–195, 2001.
6. Donald R Jones, Matthias Schonlau, and William J Welch. Efficient global optimization of expensive black-box functions. *Journal of Global optimization*, 13(4):455–492, 1998.
7. Jonas Mockus, Vytautas Tiesis, and Antanas Zilinskas. The application of bayesian methods for seeking the extremum. *Towards global optimization*, 2(117-129):2, 1978.
8. H-M Gutmann. A radial basis function method for global optimization. *Journal of global optimization*, 19(3):201–227, 2001.
9. Rommel G Regis and Christine A Shoemaker. A stochastic radial basis function method for the global optimization of expensive functions. *INFORMS Journal on Computing*, 19(4):497–509, 2007.
10. Reiner Horst and Hoang Tuy. *Global optimization: Deterministic approaches*. Springer Science & Business Media, 2013.
11. Reiner Horst and Panos M Pardalos. *Handbook of global optimization*, volume 2. Springer Science & Business Media, 2013.
12. Yaroslav D Sergeyev and Dmitri E Kvasov. Global search based on efficient diagonal partitions and a set of lipschitz constants. *SIAM Journal on Optimization*, 16(3):910–937, 2006.
13. Aimo Törn and Antanas Žilinskas. *Global optimization*. Springer, 1989.
14. János D Pintér. *Global optimization in action: continuous and Lipschitz optimization: algorithms, implementations and applications*, volume 6. Springer Science & Business Media, 1995.
15. Remigijus Paulavičius and Julius Žilinskas. Analysis of different norms and corresponding lipschitz constants for global optimization in multidimensional case. *Information Technology and Control*, 36(4), 2007.
16. Bruno O Shubert. A sequential method seeking the global maximum of a function. *SIAM Journal on Numerical Analysis*, 9(3):379–388, 1972.
17. Regina Hunter Mladineo. An algorithm for finding the global maximum of a multimodal, multivariate function. *Mathematical Programming*, 34(2):188–200, 1986.
18. D.R. Jones, C.D. Perttunen, and B.E. Stuckman. Lipschitzian optimization without the Lipschitz constant. *Journal of Optimization Theory and Applications*, 79(1):157–181, 1993.
19. J. M. Gablonsky and C. T. Kelley. A locally-biased form of the direct algorithm. *J. of Global Optimization*, 21(1):27–37, September 2001.
20. Jonas Mockus. On the pareto optimality in the context of lipschitzian optimization. *Informatika*, 22(4):521–536, 2011.

21. Remigijus Paulavičius, Yaroslav D Sergeyev, Dmitri E Kvasov, and Julius Žilinskas. Globally-biased direct algorithm with local accelerators for expensive global optimization. *Expert Systems with Applications*, 144:113052, 2020.
22. Jonas Mockus, Remigijus Paulavičius, Dainius Rusakevičius, Dmitrij Šešok, and Julius Žilinskas. Application of reduced-set pareto-lipschitzian optimization to truss optimization. *Journal of Global Optimization*, 67(1-2):425–450, 2017.
23. Qunfeng Liu, Jinping Zeng, and Gang Yang. Mrdirect: a multilevel robust direct algorithm for global optimization problems. *Journal of Global Optimization*, 62(2):205–227, 2015.
24. Qunfeng Liu, Guang Yang, Zhongzhi Zhang, and Jinping Zeng. Improving the convergence rate of the direct global optimization algorithm. *Journal of Global Optimization*, 67(4):851–872, 2017.
25. Daniela Lera and Yaroslav D Sergeyev. Deterministic global optimization using space-filling curves and multiple estimates of lipschitz and hölder constants. *Communications in Nonlinear Science and Numerical Simulation*, 23(1-3):328–342, 2015.
26. Remigijus Paulavičius and Julius Žilinskas. Simplicial lipschitz optimization without lipschitz constant. In *Simplicial Global Optimization*, pages 61–86. Springer, 2014.
27. Yaroslav D Sergeyev. An information global optimization algorithm with local tuning. *SIAM Journal on Optimization*, 5(4):858–870, 1995.
28. Roman G Strongin. Algorithms for multi-extremal mathematical programming problems employing the set of joint space-filling curves. *Journal of Global Optimization*, 2(4):357–378, 1992.
29. Yaroslav D Sergeyev, Roman G Strongin, and Daniela Lera. *Introduction to global optimization exploiting space-filling curves*. Springer Science & Business Media, 2013.
30. Dmitri E Kvasov, Clara Pizzuti, and Yaroslav D Sergeyev. Local tuning and partition strategies for diagonal go methods. *Numerische Mathematik*, 94(1):93–106, 2003.
31. Victor Gergel, Vladimir Grishagin, and Ruslan Israfilov. Local tuning in nested scheme of global optimization. *Procedia Computer Science*, 51:865–874, 2015.
32. Victor Gergel, Vladimir Grishagin, and Alexander Gergel. Adaptive nested optimization scheme for multidimensional global search. *Journal of Global Optimization*, 66(1):35–51, 2016.
33. Victor P Gergel. A global optimization algorithm for multivariate functions with lipschitzian first derivatives. *Journal of Global Optimization*, 10(3):257–281, 1997.
34. Donald R Jones and Joaquim RRA Martins. The direct algorithm: 25 years later. *Journal of Global Optimization*, pages 1–46, 2020.
35. Giampaolo Liuzzi, Stefano Lucidi, and Veronica Piccialli. A direct-based approach exploiting local minimizations for the solution of large-scale global optimization problems. *Computational Optimization and Applications*, 45(2):353–375, 2010.
36. Giampaolo Liuzzi, Stefano Lucidi, and Veronica Piccialli. Exploiting derivative-free local searches in direct-type algorithms for global optimization. *Computational Optimization and Applications*, 65(2):449–475, 2016.
37. Richard H Byrd, Peihuang Lu, Jorge Nocedal, and Ciyou Zhu. A limited memory algorithm for bound constrained optimization. *SIAM Journal on scientific computing*, 16(5):1190–1208, 1995.
38. S. Lucidi and M. Sciandrone. A derivative-free algorithm for bound constrained optimization. *Computational Optimization and Applications*, 21(2):119–142, 2002.

39. Momin Jamil and Xin She Yang. A literature survey of benchmark functions for global optimisation problems. *International Journal of Mathematical Modelling and Numerical Optimisation*, 4(2):150, 2013.
40. Fabio Schoen. A wide class of test functions for global optimization. *Journal of Global Optimization*, 3(2):133–137, 1993.
41. Marco Gaviano, Dmitri E. Kvasov, Daniela Lera, and Yaroslav D. Sergeyev. Software for generation of classes of test functions with known local and global minima for global optimization, 2011.
42. Gianni Di Pillo, Giampaolo Liuzzi, Stefano Lucidi, Veronica Piccialli, and Francesco Rinaldi. A direct-type approach for derivative-free constrained global optimization. *Computational Optimization and Applications*, 65(2):361–397, 2016.
43. Danny D'Agostino, Andrea Serani, and Matteo Diez. On the combined effect of design-space dimensionality reduction and optimization methods on shape optimization efficiency. In *19th AIAA/ISSMO Multidisciplinary Analysis and Optimization Conference (MA²O), AVIATION 2018*, Atlanta, GA, USA, June 25-29, 2018.
44. Nikolaus Hansen, Anne Auger, Raymond Ros, Steffen Finck, and Petr Pošík. Comparing results of 31 algorithms from the black-box optimization benchmarking bbob-2009. In *Proceedings of the 12th annual conference companion on Genetic and evolutionary computation*, pages 1689–1696, 2010.
45. Andrea Cassioli and Fabio Schoen. Global optimization of expensive black box problems with a known lower bound. *Journal of Global Optimization*, 57(1):177–190, 2013.
46. Momin Jamil and Xin She Yang. A literature survey of benchmark functions for global optimisation problems. *International Journal of Mathematical Modelling and Numerical Optimisation*, 4(2):150, 2013.
47. Roman G Strongin and Yaroslav D Sergeyev. *Global optimization with non-convex constraints: Sequential and parallel algorithms*, volume 45. Springer Science & Business Media, 2013.
48. Elizabeth D Dolan and Jorge J Moré. Benchmarking optimization software with performance profiles. *Mathematical programming*, 91(2):201–213, 2002.